Cerebral Cortex, December 2018;28: 4179–4194

doi: 10.1093/cercor/bhx273
Advance Access Publication Date: 9 November 2017
Original Article

ORIGINAL ARTICLE

Meta-Connectomic Analysis Reveals Commonly Disrupted Functional Architectures in Network Modules and Connectors across Brain Disorders

Zhiqiang Sha[1,2,3], Mingrui Xia[1,2,3], Qixiang Lin[1,2,3], Miao Cao[1,2,3], Yanqing Tang[4,5], Ke Xu[6], Haiqing Song[7], Zhiqun Wang[8,9], Fei Wang[4,5,6], Peter T. Fox[10,11,12,13], Alan C. Evans[14] and Yong He[1,2,3]

[1]National Key Laboratory of Cognitive Neuroscience and Learning, Beijing Normal University, Beijing 100875, China, [2]Beijing Key Laboratory of Brain Imaging and Connectomics, Beijing Normal University, Beijing 100875, China, [3]IDG/McGovern Institute for Brain Research, Beijing Normal University, Beijing 100875, China, [4]Department of Psychiatry, The First Affiliated Hospital of China Medical University, Shenyang, Liaoning, 110001, China, [5]Brain Function Research Section, The First Affiliated Hospital of China Medical University, Shenyang, Liaoning 110001, China, [6]Department of Radiology, The First Affiliated Hospital of China Medical University, Shenyang, Liaoning 110001, China, [7]Department of Neurology, Xuanwu Hospital of Capital Medical University, Beijing 100053, China, [8]Department of Radiology, Xuanwu Hospital of Capital Medical University, Beijing 100053, China, [9]Department of Radiology, Dongfang Hospital, Beijing University of Chinese Medicine, Beijing 100078, China, [10]Research Imaging Institute, University of Texas Health Science Center at San Antonio, TX 78229, USA, [11]Department of Radiology, University of Texas Health Science Center at San Antonio, TX 78229, USA, [12]South Texas Veterans Health Care System at San Antonio, TX 78229, USA, [13]Shenzhen University School of Medicine, Shenzhen 518061, China and [14]McConnell Brain Imaging Center, Montreal Neurological Institute, Montreal, QC, Canada H3A2B4

Address correspondence to Yong He, National Key Laboratory of Cognitive Neuroscience and Learning, Beijing Key Laboratory of Brain Imaging and Connectomics, IDG/McGovern Institute for Brain Research, Beijing Normal University, China. Email: yong.he@bnu.edu.cn

Zhiqiang Sha and Mingrui Xia contributed equally to this work

Abstract

Neuropsychiatric disorders are increasingly conceptualized as disconnection syndromes that are associated with abnormal network integrity in the brain. However, whether different neuropsychiatric disorders show commonly dysfunctional connectivity architectures in large-scale brain networks remains largely unknown. Here, we performed a meta-connectomic study to identify disorder-related functional modules and brain regions by combining meta-analyses of 182 published resting-state functional MRI studies in 11 neuropsychiatric disorders and graph-theoretical analyses of 3 independent resting-state functional MRI datasets with healthy and diseased populations (Alzheimer's disease and major depressive disorder [MDD]). Three major functional modules, the default mode, frontoparietal, and sensorimotor networks were commonly abnormal across disorders. Moreover, most of the disorders preferred to target the network connector nodes that were primarily involved in intermodule communications and multiple cognitive components. Apart from these common dysfunctions, different brain disorders were associated with specific alterations in network modules and connector regions.

Finally, these meta-connectomic findings were confirmed by two empirical example cases of Alzheimer's disease and MDD. Collectively, our findings shed light on the shared biological mechanisms of network dysfunctions of diverse disorders and have implications for clinical diagnosis and treatment from a network perspective.

Key words: connectomics, connector, meta-analysis, module, resting-state fMRI

Introduction

The human brain is considered as a highly dynamic, complex network that supports highly efficient information processing across the regions and underlies cognition and behavior. In the past decade, graph-theoretical analyses of healthy human brain networks have identified nontrivial topological properties, such as a highly modularized architecture (He et al. 2009; Meunier et al. 2009; Bressler and Menon 2010; Power et al. 2011) and densely connected hubs (Achard et al. 2006; Buckner et al. 2009; Liang et al. 2013; van den Heuvel and Sporns 2013a). Modules, which are presumably shaped by evolutionary constraints such as the rules of economic trade-off between the wiring costs and global efficiency (Newman and Girvan 2004; Bullmore and Sporns 2012), are crucial for ensuring efficient information propagation across the whole network. Several studies have indicated that brain modules such as the default mode network (DMN), fronto-parietal network (FPN), and sensorimotor network (SMN) are engaged in discrete cognitive functions (Bertolero et al. 2015) and in adaptation to the rapidly changing outside environment (Bassett and Gazzaniga 2011; Deco et al. 2011; Liang et al. 2016). Relating to modules, network connectors are the nodes that densely connect with distinct modules and serve critical roles in coordinating network integrity (He et al. 2009; Power et al. 2013). These connectors are primarily concentrated in the association cortex and limbic/paralimbic regions that support multiple cognitive processes (Cole et al. 2013; Warren et al. 2014; Bertolero et al. 2015; Liang et al. 2016). Studying networked modules and connectors in the brain is deepening our understanding of the working mechanisms of cognitive processing in health and disease.

Neuropsychiatric disorders and their responses to clinical treatments are typically associated with changes in cognitive processing, which are usually accompanied by alterations in both structural and functional brain networks. On the structural side, for example, patients with Alzheimer's disease (AD) and major depressive disorder (MDD) exhibit gray matter loss in regions of the DMN and FPN (Bozzali et al. 2006; Frodl et al. 2008; He et al. 2008; Seeley et al. 2009; van Tol et al. 2010; Schmaal et al. 2017); patients with MDD and Parkinson's disease (PD) manifest structural restorations in regions of the FPN, DMN and SMN after exposure to drug treatment and stimulated intervention (van Hartevelt et al. 2014; Yoon et al. 2016; Qin et al. 2017). Intriguingly, Crossley et al. (2014) performed a meta-analysis of structural MRI data in 26 brain disorders and showed that gray matter atrophy in most disorders is mainly located in the regions of the DMN, FPN, and SMN that are evident in brain hubs. On the functional side, resting-state functional MRI (R-fMRI), a noninvasive functional imaging technique that captures spontaneous or intrinsic brain activity based on the blood oxygen level-dependent signal, provides unique opportunities to explore functional network abnormalities in brain disorders (Biswal et al. 1995; Fox et al. 2005; Wang et al. 2010). Particularly for psychiatric disorders without obvious organic pathological alterations (e.g., MDD and schizophrenia), subtle brain changes could be sensitively detected by R-fMRI (Catani and ffytche 2005; Filippi et al. 2013; Fornito et al. 2015; Gong and He 2015). Recently, many R-fMRI studies have indicated disrupted functional architectures in various brain disorders involving modules and connectors (Menon 2011; Fornito et al. 2015; Gong and He 2015; Sporns and Betzel 2016). It needs to be emphasized that functional brain networks are considered crucial to elucidating the neurophysiological dynamics, which cannot be fully mirrored by structural features. Moreover, the therapeutic effects of drug administration and brain stimulation represent shared functional remodeling of the regions involving the DMN, FPN, and SMN across diverse psychiatric and neurological disorders (McIntyre and Hahn 2010; Fox et al. 2012, 2014), which suggests a possible convergent disruptive pattern. To date, the existence of commonly abnormal functional architectures in brain networks across various neuropsychiatric disorders remains largely unknown. In particular, there is an urgent push to investigate whether selective dysfunctions of functional modules and node types are partially shared across disorders, which will extend our understanding of the biological mechanisms underlying such disorders and will have implications for clinical treatments that can provide therapeutic benefits.

To address these issues, we performed a meta-connectomic study by combining meta-analyses involving 182 published R-fMRI studies in 11 brain disorders and graph-theoretical network analyses on 3 independent R-fMRI datasets with healthy and diseased populations. Specifically, we searched R-fMRI neuropsychiatric studies that assessed between-group differences with whole-brain functional analysis to understand the shared and different patterns of functional abnormalities across disorders, as well as their roles in global communication in terms of network modules and connectors. In this study, we aimed to (1) determine whether distinct brain disorders exhibit common and specific network dysfunctions in modular architectures, as reflected by spontaneous neuronal activity measured from the R-fMRI meta-analysis; (2) if so, determine whether these disorders selectively target the connectors with denser intermodule connections that support multiple cognitive processes (Bertolero et al. 2015); and (3) finally, validate the previously described meta-analysis results based on brain network analysis of two independent R-fMRI datasets (AD and MDD).

Materials and Methods

Meta-Analysis of R-fMRI Studies in Brain Disorders

Study Selection Criteria

To include as many brain disorders as possible, we selected the disorders described in Chapters V and VI of the 10th Edition of the International Classification of Disorders (ICD-10, 2010) and performed searches in PubMed (PubMed Central), the BrainMap database, ScienceDirect, Web of Science, and Neurosynth (Supplementary Fig. S1). These included studies were restricted to those with whole-brain R-fMRI analyses without a prior selection in regions of interest using the amplitude of low-frequency fluctuations (ALFF) (Zang et al. 2007), regional homogeneity (Zang et al. 2004), independent component analysis

(Smith et al. 2009), or voxel-based functional network degree (or strength) analysis (Buckner et al. 2009; Liang et al. 2013). These metrics reflect the coordination of brain activities ranging from a very short to long distance. ALFF reflects the fluctuated amplitude of the synchronization among a population of neurons within a voxel; regional homogeneity evaluates similarities in activities between neighboring voxels; independent component analysis reveals tight correlations between different voxels in the same functional system; and finally, voxel-based degree (strength) explores the integration between a given voxel and all the others of the whole brain. Therefore, in our meta-analysis, these metrics were combined together to explore abnormalities in functional coordination in brain disorders. To this end, we selected 182 R-fMRI studies of 11 brain disorders, involving 6683 patients and 6692 normal controls in total (Supplementary Fig. S2). The 11 brain disorders comprised AD, attention deficit hyperactivity disorder (ADHD), autism spectrum disorder (ASD), bipolar disorder (BD), depressive disorder (DPD), mild cognitive impairment (MCI), multiple sclerosis (MS), obsessive-compulsive disorder (OCD), PD, post-traumatic stress disorder (PTSD), and schizophrenia (SCZ) (Table 1). For details regarding study selection criteria, see the Supplementary Methods.

ALE Meta-Analysis

For each published R-fMRI study, we extracted the reported coordinates for which between-group differences existed. The coordinates in the Talairach space were converted to the Montreal Neurological Institute (MNI) space using the tal2icbm transformation (Lancaster et al. 2007). Notably, these coordinates were divided into 2 categories based on the direction of the effects (e.g., lower and higher activity in patients with brain disorders compared with that in healthy controls) and were used separately in subsequent activation likelihood estimation (ALE) analyses.

To identify disorder-related regions across R-fMRI studies, the ALE analysis was performed using GingerALE software (www.brainmap.org/ale/, version 2.3.3). The ALE represents a coordinate-based meta-analysis of neuroimaging studies, and it treats reported foci as an uncertainty distribution (Eickhoff et al. 2012). In the ALE, foci were modeled as a spatial 3D Gaussian probability distribution. For each study, we generated a modeled activation map by converting foci into probability distributions. The convergence of all modeled activation maps across studies was subsequently used to obtain voxel-wise ALE scores by estimating the uncertain peaks, which reflect the union of activation probabilities across experiments. The significance threshold was set at $P < 0.05$ (FDR corrected) with a cluster size of 200 mm^3.

Meta-Analytic Maps

Using the ALE maps from the previously described meta-analysis, we generated three types of abnormal maps, including disorder-specific maps, disorder-general maps, and disorder-conjunction maps. Briefly, we obtained disorder-specific maps (lower and higher activity, which represented functional activity abnormalities) by performing an ALE meta-analysis for the included studies of each disorder. Disorder-general maps were subsequently created by performing an ALE meta-analysis of the studies in which the same number of R-fMRI studies were randomly extracted from each disorder and further pooled together. Notably, 7 studies of lower activity and 6 studies of higher activity were randomly extracted because of the lowest number of reports on these disorders. This randomized procedure was performed 100 times. To reduce the effects of different sample sizes among studies, for each disorder, we used the following equation (Crossley et al. 2014):

$$Cs = Ns \times \frac{\min(Ncs)}{Ncs} \quad (1)$$

where Cs indicates the corrected sample size, *Ns* indicates the original number of patients reported in one specific study, *Ncs* indicates all subjects in one disorder selected for analysis, and min(*Ncs*) indicates the minimum number of subjects included in randomly selected studies of one disorder. We defined disorder-general maps (lower and higher activity) as the mean maps of 100 meta-analytic results. The disorder-general maps characterized the common abnormality across all brain disorders. Finally, to validate our meta-analytic findings from the perspective of the frequencies of abnormal brain regions across disorders, we generated disorder-conjunction maps (lower and higher activity). For each disorder, the disorder-specific maps derived from the ALE meta-analysis were binarized and subsequently overlapped across disorders to calculate the abnormal frequencies in a voxel-wise manner. The resultant images were spatially smoothed with a 4-mm full-width at half-maximum Gaussian kernel using SPM8.

Graph-Theory Connectomic Analysis of Real R-fMRI Data

Dataset Overview and Image Preprocessing

The following independent R-fMRI datasets were included in our studies (Table 2): Dataset 1 with R-fMRI data of 146 healthy

Table 1. Number of studies, patients and controls included in the meta-analysis.

Brain disorders	Abbr.	Studies (*N*)	Patients (*N*)	Controls (*N*)
Alzheimer's disease	AD	17	472	520
Attention deficit hyperactivity disorder	ADHD	9	485	473
Autism spectrum disorder	ASD	8	412	476
Bipolar affective disorder	BD	10	404	478
Depressive disorder	DPD	32	817	806
Mild cognitive impairment	MCI	23	630	570
Multiple sclerosis	MS	10	387	274
Obsessive-compulsive disorder	OCD	11	279	318
Parkinson's disease	PD	25	892	683
Post-traumatic stress disorder	PTSD	8	214	232
Schizophrenia	SCZ	29	1691	1862
Total		182	6683	6692

Table 2. R-fMRI Datasets and Demographics included in this study.

	Meta-Dataset		Dataset 1	Dataset 2		Dataset 3	
	Patients	Controls	Healthy	AD	Controls	MDD	Controls
Subjects (N)	6683	6692	143	32	38	108	183
Gender (N, male/female)	3356/2777[a]	3162/2978[a]	69/74	14/18	13/25	35/73	73/110
Age (years, mean ± std)	39.45 ± 19.43[b]	38.76 ± 19.00[b]	22.89 ± 2.27	71.25 ± 8.63	68.39 ± 7.78	25.75 ± 8.51	26.62 ± 8.00

AD, Alzheimer's disease; MDD, major depressive disorder; std, standard deviation.
[a]Gender information was extracted from available 173 studies by summing up the exact numbers in each study.
[b]Age information was extracted by averaging the mean and standard deviation values across 179 studies.

subjects, Dataset 2 with R-fMRI data of 32 AD patients, and 38 healthy controls and Dataset 3 with R-fMRI data of 114 MDD patients and 189 healthy controls. Written informed consent was obtained from each participant. The study designs of Datasets 1–3 were approved by the Institutional Review Board of the State Key Laboratory of Cognitive Neuroscience and Learning at the Beijing Normal University, the Medical Research Ethics Committee of Xuanwu Hospital and the Institutional Review Board of the China Medical University, respectively. Notably, Dataset 1 was used to identify healthy functional brain systems which that served as a normal template to investigate the spatial distribution of disorder-related regions from the meta-analysis. Datasets 2 and 3 were used to confirm whether the AD and MDD-related functional abnormalities identified via the meta-analysis were observed by using brain network analysis in experimental data, respectively. All R-fMRI data (Datasets 1, 2, and 3) were preprocessed using a standardized procedure, and the resultant data were used for network construction and analyses. Data of 3 subjects from Dataset 1 and 12 subjects from Dataset 3 (6 MDD patients and 6 controls) were discarded due to large head motion. For details regarding the participants, scanning parameters and preprocessing steps of these datasets, see the Supplementary Methods and Supplementary Tables (Table S1 and S2).

Construction of Voxel-Wise Functional Brain Network

For the three datasets (Datasets 1, 2, and 3), we used identical methods to construct the voxel-wise brain functional networks. Briefly, we initially defined network nodes as 45 381 gray matter voxels that were derived from the automated anatomical labeling atlas (Tzourio-Mazoyer et al. 2002). For each subject, we subsequently generated an individual functional connectivity matrix by computing Pearson correlations between the preprocessed time courses of every pair of voxels, which resulted in a symmetric 45 381 × 45 381 correlation matrix for each individual. We restricted the following analyses to positive edges and set negative edges to 0 due to their biologically ambiguous interpretations (Schwarz and McGonigle 2011).

Meta-Connectomic Analysis: Modules

i) Modular identification in healthy brain networks (Dataset 1). A well-known 7-system parcellation was provided by Yeo et al. (Yeo et al. 2011); however, the system division did not include subcortical regions. Given the potential importance of subcortical regions in neuropsychiatric disorders, we identified the functional modules in healthy brain networks based on an independent dataset. Briefly, we constructed a group-level brain network by thresholding the averaged correlation matrix that was obtained from a set of correlation matrices in the group of healthy subjects (N = 143). A network density threshold of 5% was selected to ensure the sparsity nature of the brain network and simultaneously remove weak correlations. Here, we adopted the Newman algorithm for modular detection (Newman and Girvan 2004). The modularity $Q(p)$ for a specific partition p was defined as follows:

$$Q(p) = \sum_{s=1}^{N_m} \left[\frac{l_s}{L} - \left(\frac{d_s}{2L} \right)^2 \right] \quad (2)$$

where N_m is the number of modules, L is the number of connections in the network, l_s is the number of connections between nodes in module s, and d_s is the sum of the degrees of the nodes in module s. The largest value of Q with the optimal number of modules was selected for further investigation. Notably, after automatically detecting functional modules, we manually combined some smaller modules into a larger one (e.g., combining the anterior and posterior DMN modules into a single DMN module) according to the functional parcellations of Yeo et al.

ii) Spatial distribution of disorder-related regions with meta-analysis in healthy brain network modules. Briefly, for each disorder-specific ALE map (lower and higher activity), we initially computed the number of disorder-affected voxels within each of the previously identified 7 modules. We subsequently determined the ratio between the number of affected voxels within each module and the number of all affected voxels within the disorder-specific map. Thus, we obtained the proportions of disorder-related regions within modules.

Meta-Connectomic Analysis: Connectors

i) Different roles of brain nodes in healthy brain networks (Dataset 1). To investigate the nodal roles in intra- and inter-modular communications, we measured the within-module degree (WMD) and the participant coefficient (PC) in the healthy brain network as follows. The following WMD z-score measures how well nodes are connected within modules:

$$z_i = \frac{k_i - \overline{k_s}}{\sigma_s} \quad (3)$$

where k_i is the number of intra-modular connections of a node i within module s, k_s is the average number of intra-modular connections of all nodes in module s, and σ_s is the SD of the number of intra-modular connection of all nodes in module s (Guimera and Nunes Amaral 2005). The PC measures the level of intra-modular connectivity versus inter-modular connectivity of a node as follows:

$$PC_i = 1 - \sum_{m=1}^{N_m} \left(\frac{k_{im}}{k_i} \right)^2 \quad (4)$$

where N_m is the number of modules, k_i is the degree of node i, and k_{im} is the number of connections from node i to module m (Guimera and Nunes Amaral 2005).

All nodes were divided into the following types according to their WMD z-score and PC values, which reflected their different roles in inter- and intra-modular communication: "connector hubs", higher WMD z-scores ($z > 0$) and higher PC values ($PC \geq 0.3$); "satellite connectors", lower WMD z-scores ($z < 0$) and higher PC values ($PC \geq 0.3$); "provincial hubs", higher WMD z-scores ($z > 0$) and lower PC values ($PC < 0.3$); and "peripheral nodes", lower WMD z-scores ($z < 0$) and lower PC values ($PC < 0.3$). The former 2 types of nodes play critical roles in the coordination of integrated and segregated information communication between modules (He et al. 2009; Power et al. 2011; Cole et al. 2013), whereas the latter two support specialized functions within modules (Guimera and Nunes Amaral 2005; Guimera et al. 2007).

ii) Distribution of disorder-related regions with meta-analysis in the categorized brain network nodes. Two strategies were used. First, we compared the mean nodal properties (PC values or WMD z-scores) between disorder-affected and -unaffected regions. Briefly, for a specific disorder, we first assigned the whole-brain voxels into affected and unaffected regions according to a disorder-specific ALE map (lower and higher activity). We subsequently computed the mean property values (PC values or WMD z-scores) of the two categorized regions in the healthy brain networks. An empirical distribution was obtained by randomly reallocating the whole-brain PC values (or WMD z-scores) into 2 randomized groups and calculating the mean values of the two groups 10 000 times. The 95th percentile point of the empirical distribution was used as the value to determine whether the observed group differences could occur by chance. Second, we examined the spatial distribution of disorder-affected regions (lower and higher activity) in terms of the node types. Briefly, for each disorder-specific ALE map (lower and higher activity), we first computed the number of disorder-affected voxels within each of the four nodal types previously identified. We subsequently determined the ratio between the number of affected voxels within each node type and the number of all affected voxels within the disorder-specific map. Thus, we obtained the proportions of disorder-affected regions within 4 node types. Finally, we compared the differences in the proportions among different node types using permutation test ($N = 10\,000$), and post hoc comparisons were also conducted by nonparametric permutation test ($N = 10\,000$) between each pair of the node types. Significance was determined at $P < 0.05$. Details are described in the Supplementary Methods.

Meta-Connectomic Analysis: Cognitive Function

We further investigated whether brain regions that are involved in various disorders play crucial roles in multiple cognitive functions. We initially obtained the cognitive flexibility map from Yeo et al. (2016) (https://surfer.nmr.mgh.harvard.edu/fswiki/BrainmapOntology_Yeo2015) in which each voxel represents the number of cognitive components. For a specific cognitive component, we identified all corresponding voxels in the flexibility map and subsequently averaged the frequencies of the abnormality values within the corresponding voxels in the disorder-conjunction maps. Then, we performed a Spearman correlation analysis to investigate the relationship between the regions with frequencies of abnormalities and the cognitive component number. These analyses were independently performed for lower and higher activity.

Meta-Connectomic Analysis: Meta-analysis Versus Connectomic Analysis from Real Data in Disorders

To confirm whether our meta-analytic findings are compatible with real brain network analyses, we performed the following process using real R-fMRI data (Datasets 2 and 3) of 2 brain disorders (AD and MDD) as examples. Briefly, we initially constructed voxel-based functional network matrices for each subject using the same approach as Dataset 1. We subsequently used formulas (2)–(4) to identify functional modules and compute nodal properties (PC values and WMD z-score). Individual PC and WMD maps were spatially smoothed with full-width half-maximum (FWHM) = 4 mm. Voxel-wise differences in PC or WMD values between patients (AD or MDD) and normal controls were evaluated using two sample t-tests, controlling for age and genders. The T-values in the between-group difference maps (PC and WMD) were converted to Z-values and subsequently added together to validate our meta-analysis results. The statistical significance threshold was set at the voxel-level of $P < 0.05$ and cluster level of $P < 0.05$ with Gaussian Random Fields correction.

Meta-Connectomic Analysis: Validation

To validate our major results, we examined the influences of functional metrics selection in meta-analysis and different image preprocessing and data analysis strategies in empirical data. First, to evaluate whether different functional metrics included in the meta-analysis have influences on the general spatial patterns of brain abnormalities, we conducted the following procedures. Briefly, each of the four functional metrics (i.e., ALFF, regional homogeneity, independent component analysis, and voxel-based functional network degree/strength) was excluded in turn from the meta-analysis; thus, four disorder-general maps were obtained. We evaluated the similarities of the spatial pattern between each pair of maps by using Pearson correlation analysis. This analysis was performed for both lower and higher activity. Second, to assess whether studies with global signal regression (GSR) have an impact on our meta-analytic findings, we re-performed the meta-analysis with studies without GSR in data preprocessing. Third, to examine the effects of the threshold for connector definition, we further validated our results utilizing another commonly used PC threshold (i.e., the mean PC value) (Hagmann et al. 2008; He et al. 2009). Fourth, we validated whether our main findings were influenced by selecting different connectivity density (3 and 7%) during brain network construction and by correcting head motion using a "scrubbing" procedure (Power et al. 2012). Finally, considering that a large number of studies enrolled in the current meta-analysis were related to ALFF analysis, we further assessed the consistency between the results of the meta-analysis and empirical data on ALFF in the AD and MDD datasets. For details, see the Supplementary Methods.

Results

Disorder-Related Functional Abnormality Mainly in the DMN, FPN, and SMN Modules

Based on the disorder-general maps, we first identified regions that were commonly affected across 11 brain disorders. Disorder-associated lower activities were primarily located in the posterior cingulate cortex (PCC)/precuneus (posterior DMN), dorsomedial prefrontal cortex (dmPFC), ventrolateral PFC (vlPFC), premotor cortex and striatum (lentiform and caudate

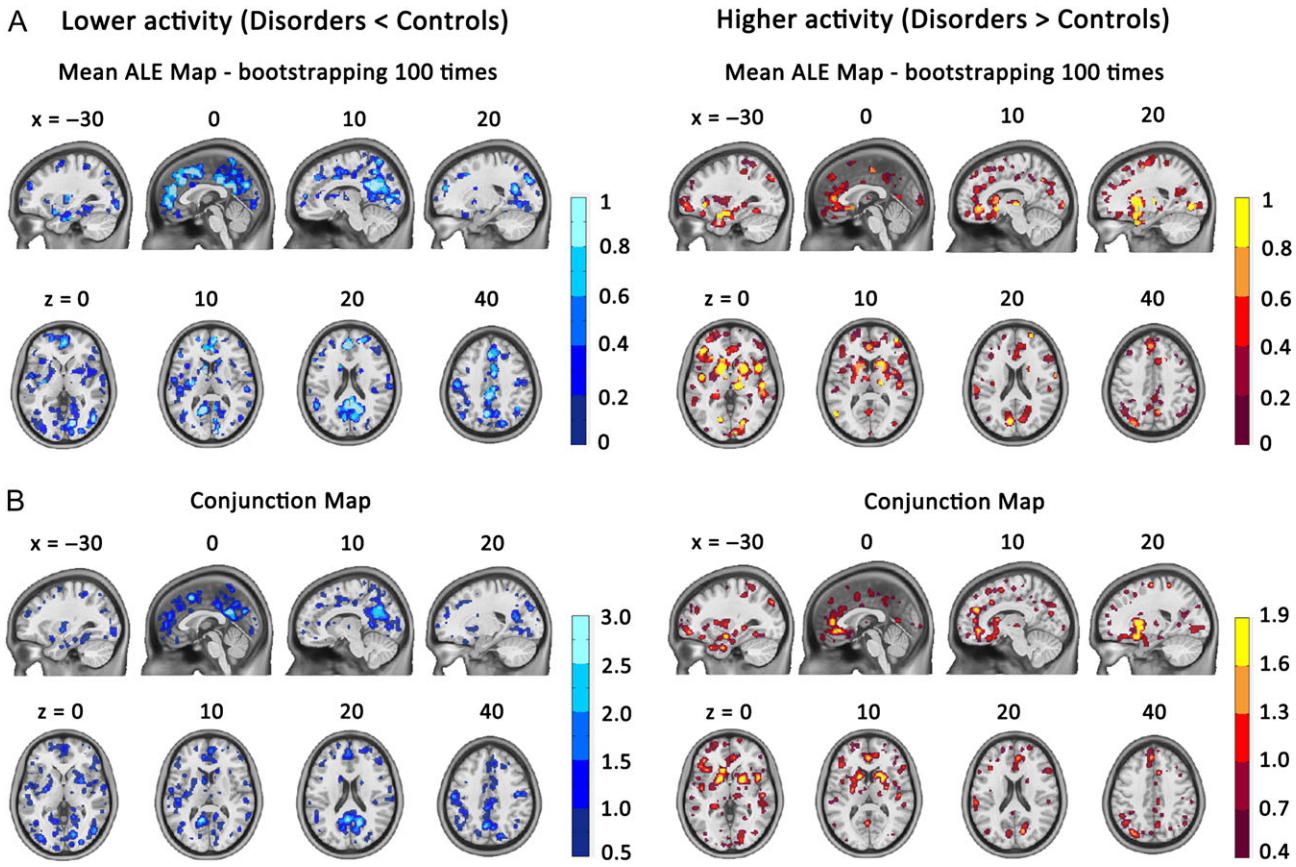

Figure 1. Distribution of disorder-related regions obtained from numerous studies of 11 brain disorders across the whole brain. (A) Disorder-general maps created by performing a meta-analysis across disorders. The left indicates the lower activity map (Disorders < Controls), and the right indicates the higher activity map (Disorders > Controls). (B) Disorder-conjunction maps obtained by overlapping disorder-specific maps. The left indicates the lower activity map, and the right indicates the higher activity map.

nucleus) (Fig. 1A). Disorder-associated higher activities were primarily located in the ventral anterior cingulate cortex (ACC) (anterior DMN), anterior insula, medial temporal cortex, supplementary motor area (SMA), and subcortical regions (e.g., the thalamus and striatum) (Fig. 1A). Moreover, the disorder-conjunction maps (Fig. 1B, Supplementary Tables S3 and S4) that were generated by calculating the frequency of abnormalities at each voxel across disorder-specific meta-analytic maps were highly similar to the disorder-general maps, indicating the high robustness of these findings. For the ALE map of each disorder, see Supplementary Figures S3 and S4.

We subsequently examined the spatial distribution of these disorder-related regions in the functional modules identified in a group of normal subjects ($N = 143$, Dataset 1). Using Dataset 1, we identified a 7-module parcellation, including the DMN, SMN, FPN, ventral attention network (VAN), dorsal attention network, visual network (VN), and limbic network (Fig. 2A). Although the proportion of the disorder-related regions varied across modules, the DMN, SMN, and FPN were commonly and highly affected across disorders (lower activity: DMN: 28.40 ± 12.11%, SMN: 17.92 ± 7.95%, FPN: 16.84 ± 4.46%; higher activity: DMN: 26.27 ± 10.05%, FPN: 18.45 ± 6.18%, SMN: 15.46 ± 9.78%) (Fig. 3A). Specifically, within the DMN, lower activity was primarily distributed in the posterior DMN (PCC/precuneus), dmPFC and ventromedial prefrontal cortex (vmPFC), but higher activity was primarily distributed in the anterior DMN (ventral ACC) and the lateral and medial temporal cortices (Supplementary Fig. S5). Within the SMN, lower activity was mainly located in the inferior premotor cortex, inferior primary somatosensory cortex, and SMA, but higher activity was located in the primary somatosensory cortex (Supplementary Fig. S5). Within the FPN, lower activity was primarily distributed in the dmPFC, temporo-parietal junction and inferior temporal cortex, but higher activity was located in the bilateral dorsolateral prefrontal cortex (dlPFC) (Supplementary Fig. S5). In addition to these common across-disorder dysfunctions in the DMN, SMN, and FPN, several other modules were targeted by specific disorders, such as lower activity in VN (18.88%) in SCZ and higher activity in the VAN (10.91%) and the VN (32.95%) in ADHD. The correspondences between each disorder and dysfunctional systems are illustrated in the circle representations (Fig. 3B).

Disorder-Related Brain Regions Concentrated in Network Connectors

To examine whether these disorder-related regions play critical roles in inter- and intra-modular communication, we computed 2 network metrics, the PC and WMD z-scores, in healthy brain functional networks (Dataset 1). Both the PC values and WMD z-scores of disorder-associated lower activity regions in the ALE map were significantly higher (both P-values < 0.001, permutation tests) than those of the other regions. For disorder-associated higher activity regions in the ALE map, the averaged PC values were significantly higher ($P < 0.001$, permutation

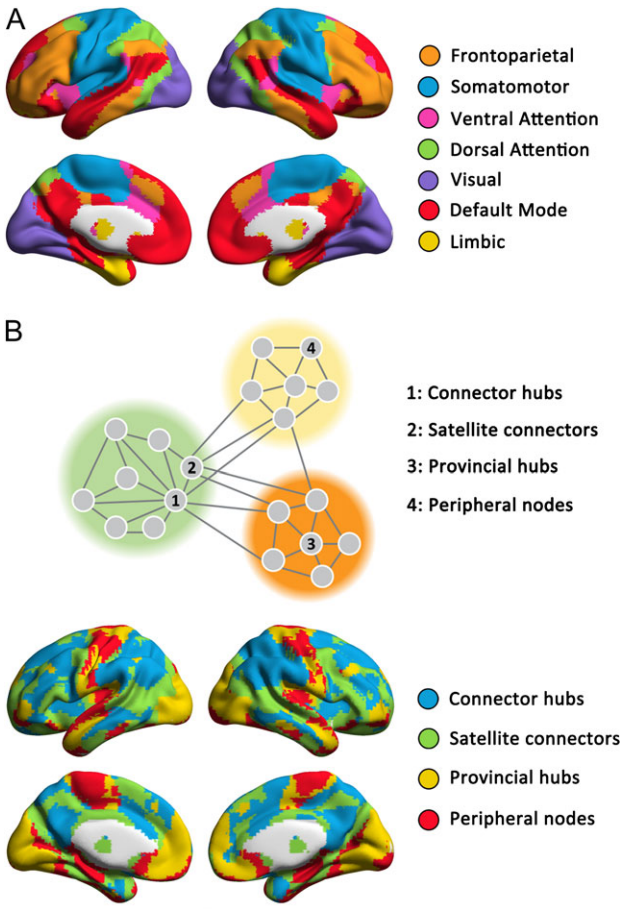

Figure 2. Spatial pattern of 7 brain systems and four node types. (*A*) Seven-network parcellation identified based on voxel-wise functional brain networks of healthy participants. Each color indicates one of the identified systems. (*B*) Illustrations of modules and four node types. Modules are represented by three colors (top). Spatial distribution of the four node types in the brain. The indexes of the nodes indicate node types corresponding to the right labels (bottom). Connector hubs in blue with PC values > 0.3 and WMD z-scores > 0; satellite connectors in green with PC values > 0.3 and WMD z-scores < 0; provincial hubs in yellow with PC values < 0.3 and WMD z-scores > 0; and the peripheral nodes in red with PC values < 0.3 and WMD z-scores < 0. The modular and node type categorization were mapped on the cortical surface using BrainNet Viewer (Xia et al. 2013).

test); however, there were nonsignificant differences in the WMD z-scores ($P = 0.48$). Similar findings were obtained for most disorder-specific ALE maps (Supplementary Fig. S6).

Subsequently, we classified all nodes into the 4 types, that is, connector hubs, satellite connectors, provincial hubs, and peripheral nodes (Fig. 2*B*). We determined that most of the putative connector nodes in the healthy brain networks were mainly located in the junctions between functionally segregated systems, which was highly similar to the conclusions of previous studies (He et al. 2009; Power et al. 2013). Importantly, disorder-related lower and higher activity regions exhibited significant differences in proportion among these 4 categories (both *P*-values < 0.001, Fig. 4*A*) as follows: lower activity: connector hubs (34.56 ± 9.10%), satellite connectors (28.14 ± 3.40%), provincial hubs (21.60 ± 6.80%), and peripheral nodes (15.71 ± 5.23%); higher activity: connector hubs (27.89 ± 7.18%), satellite connectors (32.70 ± 6.28%), provincial hubs (17.57 ± 5.88%) and peripheral nodes (21.83 ± 5.01%). We further used an additional threshold of the mean PC value to define connectors (mean PC value = 0.35) for validation purposes and found identical results (Supplementary Fig. S7). Together, the results indicated that brain disorders appear to mainly target connectors with denser intermodule connections, regardless of lower or higher activity.

To compare functionally damaged patterns across disorders, we established the PC-WMD coordinate space by mapping the averaged PC values and WMD z-scores in the lower or higher activity regions of every disorder (Fig. 4*B*). We clearly determined that nearly all brain disorders (with the exception of SCZ in lower activity and ASD and ADHD in higher activity) were associated with disrupted network connectors (connector hubs and satellite connectors), regardless of lower and higher activity regions. This result provided further support for the previously described findings. Intriguingly, each disorder occupied a specific position in the PC-WMD space. For example, AD and MCI exhibited substantially similar lower activity patterns but differed in higher activity; both ADHD and ASD shared similar lower and higher activity patterns. There were also different patterns between neurological and psychiatric disorders: the former (e.g., MCI, MS, and PD) exhibited higher PC values and WMD z-scores in lower and higher activity regions, whereas the latter (e.g., SCZ, BD, and PTSD) exhibited lower WMD z-scores in regions with higher activity.

Disorder-Related Regions were Mainly Involved in Multiple Cognitive Functions

We identified a significantly positive correlation between the probabilities of regions involving brain disorders and the number of cognitive components engaged in the tasks (lower activity: Spearman's $\rho = 0.56$, $P < 0.001$; higher activity: Spearman's $\rho = 0.79$, $P < 0.001$) (Fig. 5). This result indicated that the regions with disorder-general abnormalities tend to be involved in multiple cognitive functions.

Abnormal Functional Network Patterns using Real R-fMRI Data in AD and MDD

Voxel-based network modularity analyses in two R-fMRI data examples (AD and MDD) revealed abnormal connectivity patterns. At the modular level, we observed AD-related lower activity mainly in the DMN and SMN, MDD-related lower activity in the DMN and FPN, and AD- or MDD-related higher activity in the DMN, SMN and FPN (Supplementary Fig. S8), indicating that the three functional systems were mainly affected by AD or MDD. Additionally, we also noticed specific lower activity in the visual system in MDD.

At the nodal level, the AD patients exhibited lower activity primarily in the PCC, vmPFC/ventral ACC, supramarginal gyrus, central opercular cortex and anterior insula and higher activity mainly in the dlPFC, lateral temporal cortex, medial temporal lobe (including the hippocampus and amygdala) and primary motor cortex (Fig. 6 and Supplementary Table S5). Interestingly, several lower and higher activity regions (e.g., the vmPFC, central opercular cortex, supramarginal gyrus and frontal pole in lower activity and the medial temporal lobe, dlPFC and lateral temporal cortex in higher activity) in AD were largely compatible with our AD-specific meta-analysis findings with an overlapping percentage of 96.41% for lower activity and 90.02% for higher activity (Fig. 6). Additionally, validation analysis also revealed high consistency between the results of AD-specific meta-analysis and the abnormality identified with ALFF analysis in empirical data, with a high overlap of 94.92 and 97.10% for

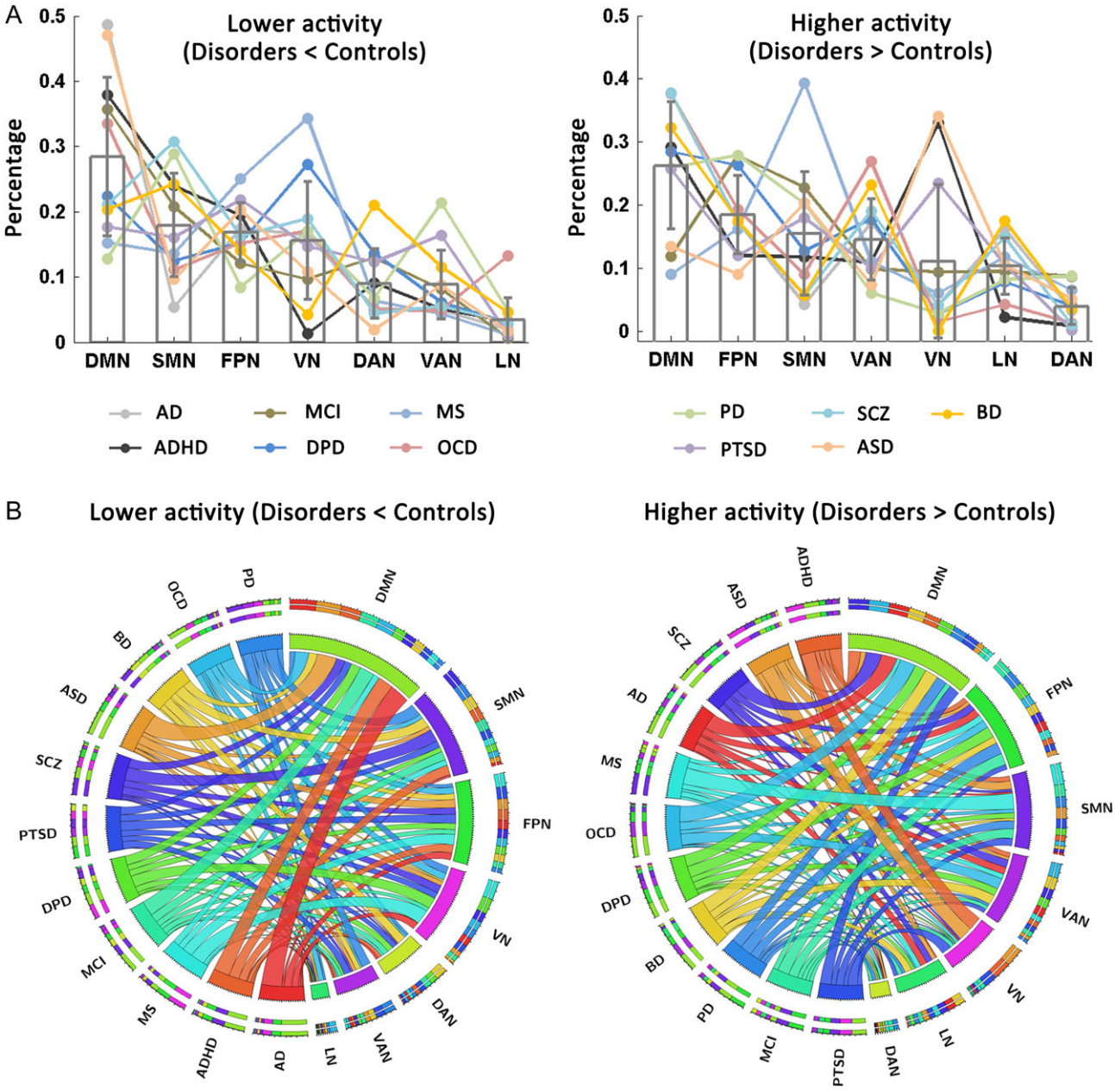

Figure 3. Distribution of disorder-related regions in the brain modules. (*A*) Plots indicate the percentages of disorder-related regions in 7 functional modules. The *x*-axis represents the modules in a decreasing order of average proportion across disorders, and the *y*-axis indicates the proportion of the disrupted regions in each module. The bar map shows the mean proportion of disrupted regions across 11 disorders in each module. The error bar represents the SD. Each color indicates one of the included disorders. (*B*) Circular representations indicate that different disorders share common and unique severely disrupted modules. Regions that exhibited lower activity (Disorders < Controls) distributed in the 7 modules are shown on the left, and regions with higher activity (Disorders > Controls) are shown on the right. The inner circular diagram indicates the relative abundance of functionally disrupted regions across disorders in the various brain modules. Each color indicates one of the modules or disorders: the modules are shown on the right side, and the 11 disorders are shown in the remaining segments of the circles. Each ribbon linked one disorder with one module. The ribbon size indicates the proportion of the abnormal regions in each individual module. The outer circles depict the relative row and column frequencies for each related segment. All information regarding the circle generation is available at http://mkweb.bcgsc.ca/tableviewer/.

lower and higher activity, respectively (Fig. 6 and Supplementary Table S6).

Likely, at the nodal level, the MDD patients exhibited lower activity mainly in the visual cortex and frontal orbital cortex and higher activity in the dlPFC; central, frontal opercular; anterior insular cortices and putamen (Fig. 7 and Supplementary Table S7). Specifically, the lower activity in the visual cortex and the higher activity in the dlPFC, vlPFC, anterior insular, and frontal operculum cortices were highly consistent with our meta-analytic findings in MDD. The overlapping ratio between the empirical abnormal regions and MDD-related meta-analytic maps reached 98.13% for lower activity and 92.53% for higher activity (Fig. 7). Additionally, we found similar patterns between the results from MDD-specific meta-analysis and from the abnormal regions identified with ALFF analysis in empirical data regardless of lower (e.g., visual

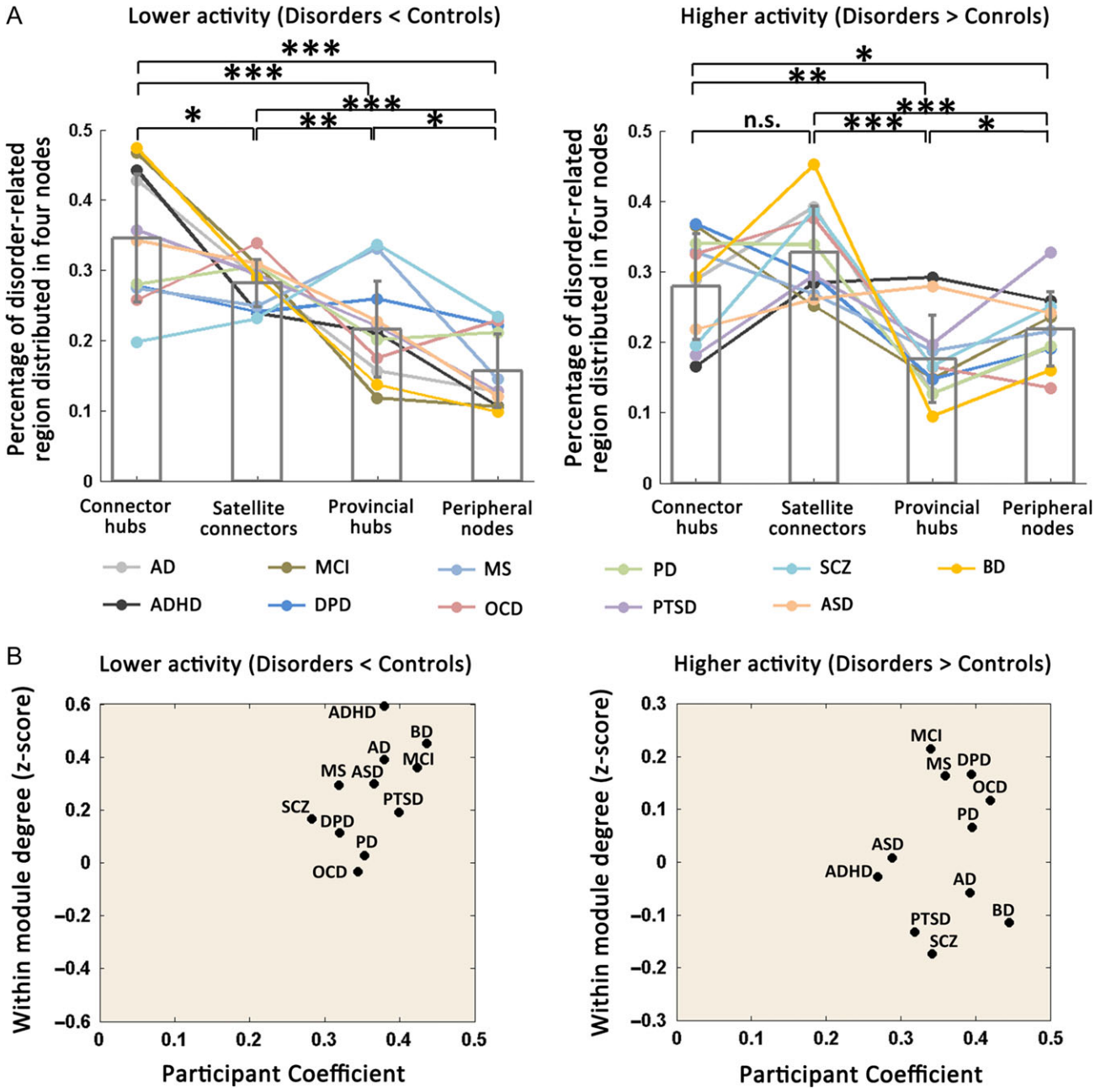

Figure 4. Distribution of disorder-related regions in four types of nodes. (*A*) Average distribution of regions with lower and higher activity in various node types across all brain disorders. The bar map indicates the mean proportion of disrupted node types across 11 disorders. The error bar represents the SD. *P < 0.05, **P < 0.01, and ***P < 0.001. The asterisks indicate significant differences between two node types. Each color indicates one of the included brain disorders. (*B*) The fingerprint maps with PC and WMD z-scores across various brain disorders. Each dot represents the average PC values and WMD z-scores of the disorder-related regions of a specific disorder. Abbreviations: AD, Alzheimer's disease; ADHD, attention deficit hyperactivity disorder; ASD, autism spectrum disorder; BD, bipolar affective disorder; DPD, depressive disorder; MCI, mild cognitive impairment; MS, multiple sclerosis; OCD, obsessive-compulsive disorder; PTSD, post-traumatic stress disorder; SCZ, schizophrenia; n.s., nonsignificant.

cortex) and higher activity (e.g., anterior insula, medial temporal lobe, and putamen) (Fig. 7 and Supplementary Table S8). The overlapping proportions between regions with ALFF differences and MDD-related meta-analytic patterns in lower and higher activity reached 99.03 and 99.53%, respectively. Finally, validation analysis in both datasets based on different network density and head motion correction generally indicated similar findings (Supplementary Figs S9 and S10).

Discussion

Using a novel meta-connectomic analysis, we showed that most brain disorders were commonly affected in several major modules, including the DMN, FPN, and SMN. Moreover, the disorder-related regions primarily concentrated in the connectors that serve as a group of nexuses that maintain intermodular communications and support multiple cognitive functions; however, different sets of connectors existed across

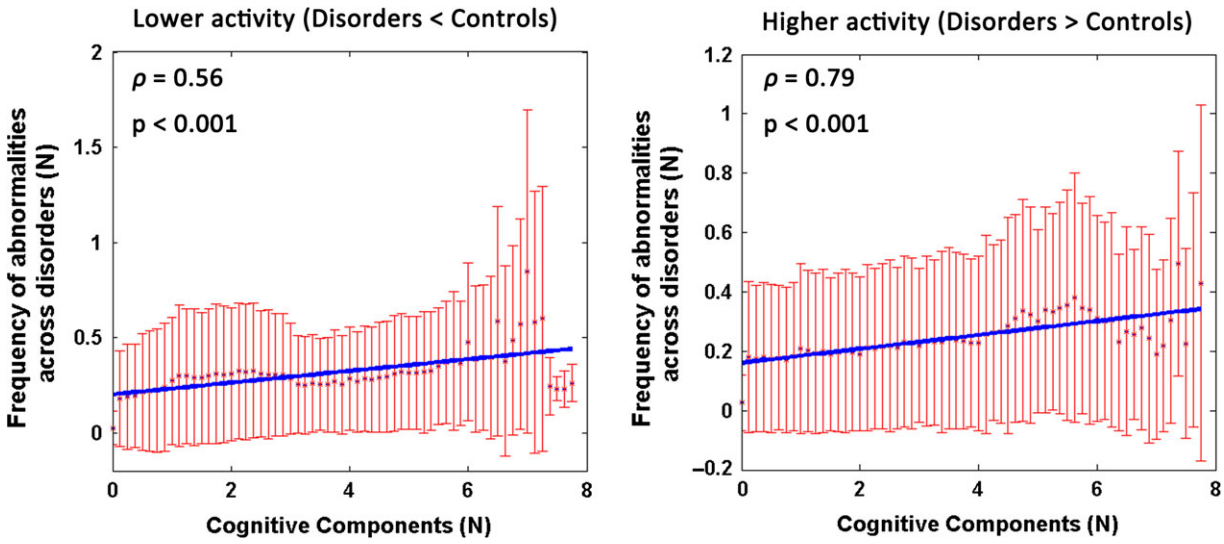

Figure 5: Relationship between the disorder-related regions and multiple cognitive functions and network robustness. Relationship between disorder-related regions and cognitive roles in tasks. The x-axis indicates the cognitive components engaged by a specific task in the functional flexibility map obtained from (Yeo et al. 2011). The y-axis indicates the averaged frequencies of abnormality across disorders of the voxels within the region. The error bar represents the SD.

disorders. Using network analysis of R-fMRI data in AD and MDD as empirical examples, we confirmed these meta-analytic findings. To the best of our knowledge, this meta-connectomic study is the first to demonstrate that different brain disorders are associated with shared alterations in the modules and connectors of functional brain networks, and the findings extend our understanding of the neural mechanisms that underlie various disorders.

Relationship Between Brain Disorders and Functional Modules

That the DMN, FPN, and SMN were commonly affected by most brain disorders. Why do these functional abnormalities often concentrate in these 3 modules? We first discussed potential explanations related to DMN and FPN dysfunctions. Abnormal cognitive functions (including memory and cognitive control) and emotional processing often appear in neuropsychiatric disorders, such as AD, MDD, and SCZ. The DMN is mainly composed of the medial prefrontal cortex, PCC and hippocampus and is involved in internal emotional processing, self-referential directed thought and memory function (Buckner et al. 2008; Anticevic et al. 2012). The FPN is mainly composed of the lateral prefrontal and parietal regions and is typically involved in cognitive control. Thus, it is not surprising to see that numerous R-fMRI studies have documented that both the DMN and FPN are associated with most mental illnesses, including AD, MDD, ASD, and SCZ (Broyd et al. 2009; Menon 2011; Agosta et al. 2012; Anticevic et al. 2012; Lynch et al. 2013; Wang et al. 2013; Baker et al. 2014). Moreover, from the perspective of energy consumption, spontaneous neuronal activity is the major factor that contributes to the cost of brain function, which may consume 20% of the body's energy budget (Raichle and Gusnard 2002; Raichle and Mintun 2006). DMN and FPN, as 2 core neurocognitive networks (Menon 2011), act as the main energy utilizer during rest (Raichle et al. 2001) and consume heavier regional cerebral blood flow and metabolisms (Liang et al. 2013; Tomasi et al. 2013). Empirical and computational modeling studies have proposed that high cost regions are frequently targeted by various disorders (de Haan et al. 2012; Crossley et al. 2014; Stam 2014). Finally, neuroimaging studies have demonstrated that the DMN and FPN modules are not only structurally connected to constitute a rich-club core brain system (Hagmann et al. 2008; van den Heuvel and Sporns 2011) but also functionally coupled to each other in task performances or the resting-state (Fox et al. 2005; Seeley et al. 2007). Thus, these works provide crucial support for commonly detected network dysfunction in the DMN and FPN across distinct disorders.

We also identified disorder-related disruption in the SMN. Many disorders were characterized by deficits in motor control, such as tremor and slowness of movement, and deficits in receiving external stimuli. The SMN was defined as the areas linked with the primary somato-motor cortex and SMA, which are used for motor skill learning and sensory perception (Biswal et al. 1995; Rioult-Pedotti et al. 1998; Butefisch et al. 2000). Thus, clinical dysfunction of sensory and motor expression would be progressively represented in the neuroimaging results. An aberrant SMN is associated with clinical symptoms and has been reported in several neuropsychiatric disorders, such as AD (Wang et al. 2007), SCZ (Keedy et al. 2009; Damaraju et al. 2014), MS (Lowe et al. 2008; Faivre et al. 2012), and PD (Wu et al. 2009). Thus, it is reasonable to observe shared disruptions in the SMN across several disorders in this study.

Recently, Fox and colleagues (Fox et al. 2014) proposed the "target-response" network to describe the close connection among stimulation sites and their target effective brain regions across diverse psychiatric and neurological disorders. Interestingly, the localization of the "target-response" network is most prominent in the DMN, SMN, and FPN, which is highly consistent with our disorder-shared functional modules. Here, we highlighted these 3 core networks identified by our meta-connectomic analysis and collectively called them the "treatment-response network". Thus, the identification of these core networks not only helps to extend the understanding of the common neurological mechanism across disorders but also provides clinical treatment guidance for therapeutic benefits at a network level.

Apart from these shared dysfunctions, some disorders also exhibited abnormal patterns in specific functional modules. For

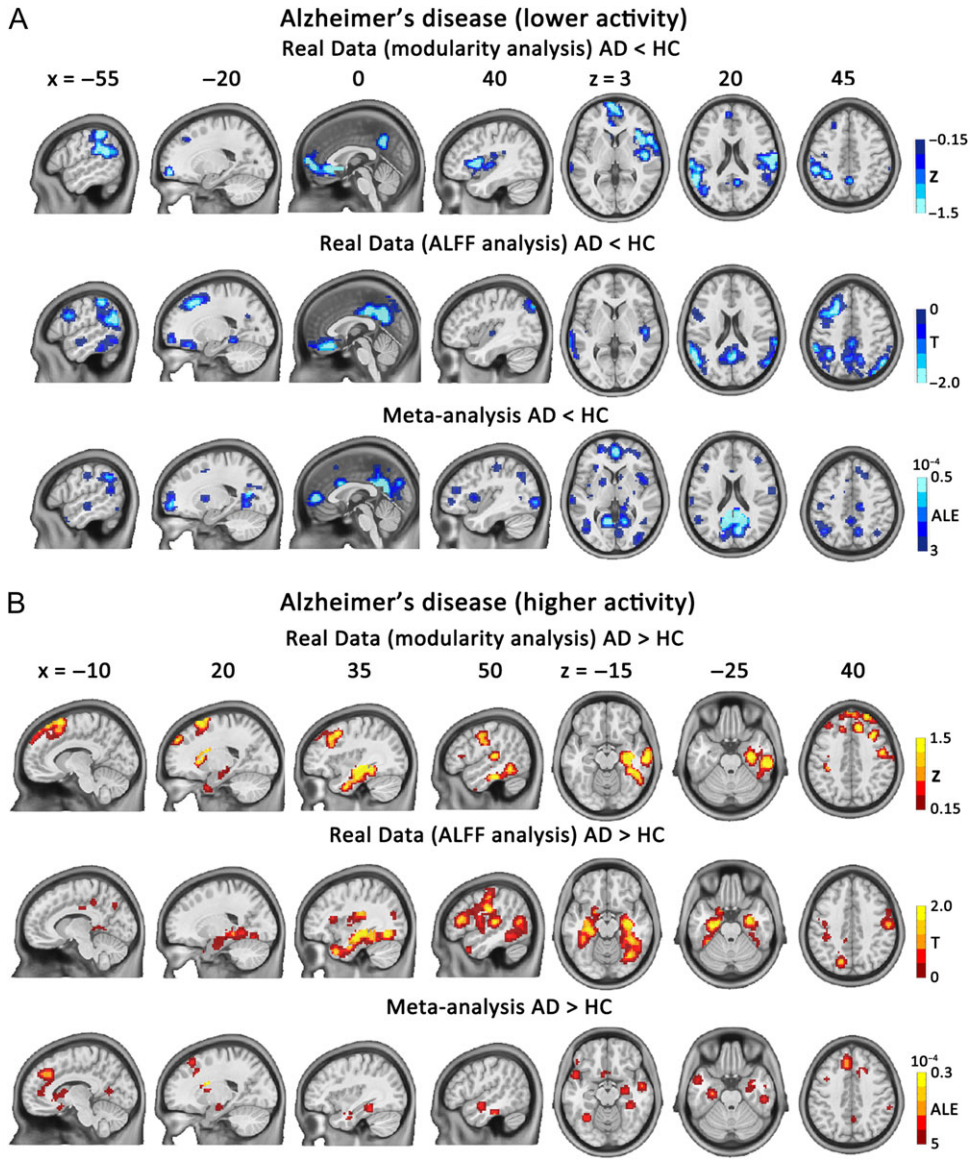

Figure 6. Comparison of AD-related abnormal regions between real data and meta-analysis data. (*A*) Whole-brain group-wise statistical maps of regions with lower activity in AD compared with the corresponding meta-analytic results. (*B*) Similar comparisons of patterns with higher activity in AD real data and the corresponding meta-analytic results are shown. Between-group difference maps for PC values and WMD z-scores were merged together for presentation. The PCC with lower activity in AD modularity analysis reached the height threshold but did not survive the cluster correction. All findings were smoothed for better visualization with FWHM = 6 mm. The color bar in the meta-analytic results represents the ALE value, whereas the Z value is presented in the real data differences among comparisons.

example, PD was observed with lower activity located partially in the VN (17.05%). Clinically, a majority of patients with PD reported visual deficits, such as misjudging objects and distances, double vision and visual perception, which was consistent with the neuroimaging results (Weil et al. 2016). These results indicated the degree to which disrupted functional systems varied across brain disorders with the exception of universally abnormal modules.

Relationship Between Brain Disorders and Network Connectors

As previously discussed, abnormal cognitive function and emotional processing are the cardinal characteristics of most neuropsychiatric disorders. Network connectors play crucial roles in coordinating inter-modular information transfer and support multiple cognitive processes (Bertolero et al. 2015; Yeo et al. 2016). To date, several R-fMRI studies have shown lower and higher connectivity in brain disorders, which are related to the connector nodes in the brain networks. For example, disrupted modular and connector communications occur in AD, and these disruptions are closely related to cognitive decline (de Haan et al. 2012; Dai et al. 2015). In stroke, focal damages to brain areas are linked to functional connectors (Gratton et al. 2012). Moreover, focal lesions in "target" connector hubs produce more severe and widespread cognitive deficits than do lesions in peripheral nodes (Warren et al. 2014). Specifically, we showed that regions that were more affected by disorders tended to be network connectors with multiple cognitive components. A recent meta-analysis study involving task-related fMRI on cognitive control revealed abnormal task-related activation in regions of the frontoparietal and salience networks,

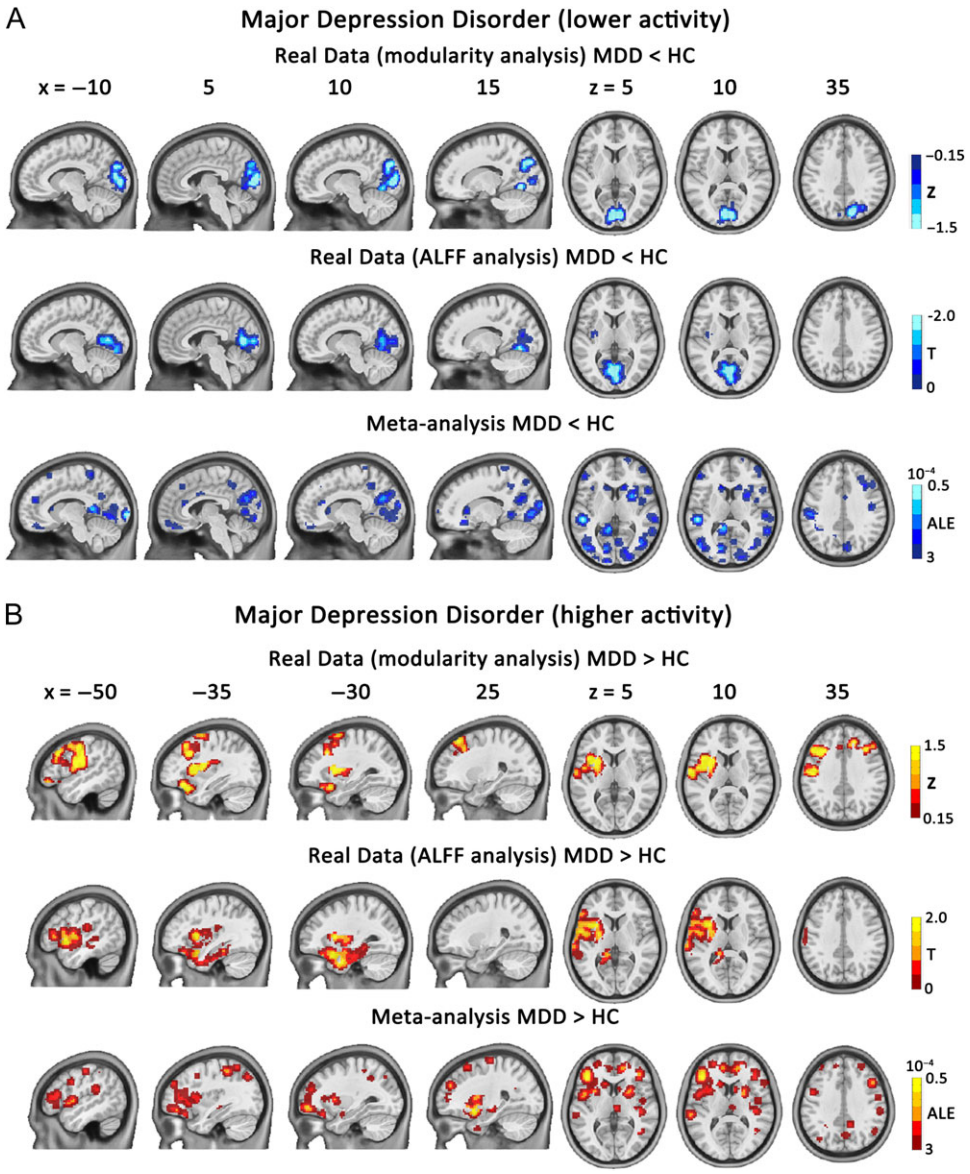

Figure 7. Comparison of MDD-related abnormal regions between real data and meta-analysis data. (*A*) Whole-brain group-wise statistical maps of regions with lower activity in MDD compared with the corresponding meta-analytic results. (*B*) Similar comparisons of patterns with higher activity in MDD real data and the corresponding meta-analytic results are shown. Between-group difference maps for PC values and WMD z-scores were merged together for presentation. All findings were smoothed for better visualization with FWHM = 6 mm. The color bar in the meta-analytic results represents the ALE value, whereas the Z value is presented in the real data differences among comparisons.

such as the dlPFC, dorsal ACC, and anterior insula, across different psychiatric disorders (McTeague et al. 2017). Many previous R-fMRI studies have suggested that these regions tend to be connectors in the functional brain networks (He et al. 2009; Power et al. 2013; Bertolero et al. 2015) and are highly in line with our results. Dysfunctions of these regions suggest a common network substrate underlying declines in cognitive processing in different brain disorders. Together, our study extended previous findings by indicating a general rule of abnormal network connectors across various neuropsychiatric disorders.

Connectors predominately lie in the association and limbic cortices that typically receive and integrate information from other sensory modalities (Mesulam 1998). The fiber tracts of neurons in the association cortex contain several million miles of axons that connect one cortex to another. In gray matter, information inputted to layer IV, in which input cells are located, was subsequently transferred to the superior (layer III) and deeper (layer V) layers, followed by integration by output cells in these two layers, where messages were integrated for output to other cerebral cortex areas (Purves et al. 2001). Moreover, research suggests that the projection neurons in adjacent cortex areas have longer and more complex dendrites and spines than those of pyramidal neurons within the primary and unimodal cortex of monkeys and humans, indicating their role in integrating more complex information in different modules (Jacobs et al. 2001; Duan et al. 2002). Thus, disruptive connectors may heavily impact the coordination of information flow across functional modules.

Notably, it was not only regions with lower activity that concentrated in the connectors, but the areas showing higher

activity did as well. We proposed two hypotheses to explain our findings, including the "radar-like" cortico-subcortical dysfunction model and compensation effects. First, previous studies have identified a cortical-basal ganglia-thalamic circuit linking cortical connectors, such as the associative cortex, limbic cortex and motor cortex, with subcortical connectors that communicates in a "radar-like" interactive manner (Bell and Shine 2016). These regions are also abnormal regardless of lower and higher activity patterns, which implicates disruption within cortical-subcortical crosstalk among brain disorders. In detail, if disorders target cortical connectors to lower activity, then subcortical connectors serve as the receptor of the "radar", representing higher activity in response to the above signals. Second, a compensation mechanism was considered in topological space. Specifically, as attacked connectors result in the decreased efficiency of inter-modular information transfer, the recruitment of the remaining connectors may be used to compensate for lower activity. Our study has plotted the "nodal fingerprint" across disorders. For example, AD and MCI exhibited severe disruptions of connector hubs in regions with lower activity and separated patterns with higher activity. These findings suggest that local compensation effects counteracted the decreased activity in other regions in the earlier stage of the progression to accomplish normal cognitive functions. However, in the later stage, the compensatory mechanism would breakdown and result in clinical behavior deficits. Finally, some of the disorders, such as PD, MCI, AD, and MS, were clustered to implicate similar abnormal patterns and provided suggestions for mechanistic understanding.

Recently, Crossley et al. (2014) proposed the hub vulnerability hypothesis in the structural connectome in most brain disorders. In the present study, we highlighted the functional connector disruption concentrated in most neuropsychiatric disorders. van den Heuvel and Sporns (2013b) determined that 86% of functional connector hubs are primarily distributed in rich-club nodes in the structural brain network, which thus indicates substantial overlap between disorder-associated functional and structural maps. However, how to explain the convergent and divergent nodes between functional and structural disruptions across different disorders remains an open question. For the shared areas, the structural networks partially shape functional connections through white matter fibers, and alterations in spontaneous brain activity, in turn, are likely to affect the structural architecture (Honey et al. 2009, 2010; Park and Friston 2013; Wang et al. 2015). Here, our results provided evidence for commonly disrupted functional patterns across disorders. Functional brain networks were considered a tool to help elucidate neurophysiological dynamics, which were not fully mirrored by structural features. Specifically, we identified higher activity patterns in the functional networks to provide a better understanding of brain dynamics across disorders, which were not shown in previous structural network studies (Crossley et al. 2014).

Consensus Findings to Validate our General Hypothesis using Network Analyses of Real R-fMRI Data

Using R-fMRI brain network analysis, we identified AD-related lower activity primarily in the vmPFC, PCC, central opercular cortex and supramarginal gyrus and higher activity primarily in the dlPFC and the medial and lateral temporal cortices. Importantly, these regions were mainly distributed in the core networks and topological connectors, which was in accordance with our meta-analytic findings. Specifically, most brain regions with lower activity correspond to cortical hubs and are spatially similar to the pattern of amyloid-β deposition revealed using positron emission tomography amyloid imaging in AD (Buckner et al. 2009). Moreover, the dlPFC, inferior temporal gyrus, parahippocampal gyrus, and lingual gyrus exhibit decreased neuronal responses during memory and semantic processing, execution function and emotional retrieval, as demonstrated by a meta-analysis (Li et al. 2015), which is compatible with our findings. The decreased nodal properties of these areas suggested their weakened roles of coordination across functional modules that corresponded to the pathological features of AD.

We implemented the R-fMRI brain network analysis to show MDD-related lower activity in the visual cortex and higher activity in the lateral PFC, anterior insula cortex and frontal operculum cortex. These findings were similar to our meta-analytic findings. The lower activity of the VN was consistent with the findings of MDD-related decreases in nodal centralities (Zhang et al. 2011). Most regions with higher activity are the main components of the FPN and DMN that have crucial roles in cognitive control, the maintenance of information in working memory and problem solving. Moreover, increased activation of these two networks has been reported during emotional control processing and working memory, implicating the disrupted communication of these networks in the brain activity of patients with DPD (Hamilton et al. 2012; Kerestes et al. 2012; Groenewold et al. 2013).

Limitations and Future Work

There are several methodological issues in the present study. First, we strove to make our search of the R-fMRI data with regard to various brain disorders as wide as possible; however, only 11 disorders were ultimately included because few R-fMRI studies met our research criteria for other disorders. In the future, additional disorders and studies must be included to further assess the robustness of our findings. Second, in our meta-analysis, we did not consider the effects of subject demographics (e.g., age, gender, and education) or clinical status (e.g., illness duration and history of drug-taking) or image preprocessing (e.g., head motion correction and removal of the global signal). Specifically, GSR is supposed to reduce global artifacts, but it can also introduce spurious anti-correlation between regions (Power et al. 2012, 2014; Murphy and Fox 2017); however, the biological mechanism for the global signal remains largely unknown. Notably, most of the studies included in our meta-analysis did not take the impact of GSR into consideration, with the exception of twelve studies that precisely reported GSR in preprocessing. Our additional meta-analysis with the remaining 170 studies without GSR revealed almost identical spatial patterns of disorder-general maps to those of our main findings (lower activity: $r = 0.92$; higher activity: $r = 0.90$; both P-values < 0.001. Supplementary Fig. S13). Thus, our findings could be mainly considered results without GSR. Given the limited number of studies with GSR, we could not assess the effects of GSR on our meta-analytic findings in the current work. Future studies involving a balanced number of processing strategies might provide valuable insights into the understanding of global signal effects. Third, in the present study, meta-analyses were separately performed with studies showing lower activity and higher activity in different brain disorders, and some of the regions exhibited both lower and higher activities. This finding was a possible outcome of the current ALE model, which can only estimate the effect in a

single direction. Some newly developed models, such as the effect-size signed differential mapping approach, provide abilities in combining both positive and negative coordinates together to obtain a unique statistic map (Radua et al. 2012, 2014). Future work adopting these models might reduce the controversy in revealing the regions with both higher and lower activities detected in ALE-based meta-analysis. Fourth, it should be noted that the disorder-related patterns identified in our meta-analysis were not exactly the same as those identified in our real dataset. One confounding factor was the sample heterogeneity in our meta-analysis created by the various subtypes of depressive disorder (e.g., recurrent, early onset, adult-onset, and medication status). Finally, we used a meta-analysis to demonstrate network dysfunctions across neuropsychiatric disorders. It would be desirable to use a real R-fMRI dataset with the same scanning and analysis procedures to compare convergent and divergent functional abnormalities across various disorders. This research would be important to identify shared and different biological mechanisms across disorders and provide novel insights into diagnostic biomarkers and treatment strategies based on across-disorder studies.

Supplementary Material

Supplementary data is available at *Cerebral Cortex* online.

Funding

The Natural Science Foundation of China (Grant Nos. 91432115, 81620108016, 91432115, 81671767, 81401479, 31521063 and 81571648), Changjiang Scholar Professorship Award (Award No. T2015027), Beijing Municipal Science & Technology Commission (Grant Nos. Z161100000216152 and Z151100003915082), Beijing Brain Project (Grant No. Z161100000216125) and Fundamental Research Funds for the Central Universities (No 2017XTCX04 and 2015KJJCA13).

Notes

We gratefully acknowledge the support of NVIDIA Corporation with the donation of the Tesla K40 GPU used for this research. *Conflict of Interest*: None declared.

References

Achard S, Salvador R, Whitcher B, Suckling J, Bullmore E. 2006. A resilient, low-frequency, small-world human brain functional network with highly connected association cortical hubs. J Neurosci. 26:63–72.

Agosta F, Pievani M, Geroldi C, Copetti M, Frisoni GB, Filippi M. 2012. Resting state fMRI in Alzheimer's disease: beyond the default mode network. Neurobiol Aging. 33:1564–1578.

Anticevic A, Cole MW, Murray JD, Corlett PR, Wang XJ, Krystal JH. 2012. The role of default network deactivation in cognition and disease. Trends Cogn Sci. 16:584–592.

Baker JT, Holmes AJ, Masters GA, Yeo BT, Krienen F, Buckner RL, Ongur D. 2014. Disruption of cortical association networks in schizophrenia and psychotic bipolar disorder. JAMA Psychiatry. 71:109–118.

Bassett DS, Gazzaniga MS. 2011. Understanding complexity in the human brain. Trends Cogn Sci. 15:200–209.

Bell PT, Shine JM. 2016. Subcortical contributions to large-scale network communication. Neurosci Biobehav Rev. 71: 313–322.

Bertolero MA, Yeo BT, D'Esposito M. 2015. The modular and integrative functional architecture of the human brain. Proc Natl Acad Sci USA. 112:E6798–E6807.

Biswal B, Yetkin FZ, Haughton VM, Hyde JS. 1995. Functional connectivity in the motor cortex of resting human brain using echo-planar MRI. Magn Reson Med. 34:537–541.

Bozzali M, Filippi M, Magnani G, Cercignani M, Franceschi M, Schiatti E, Castiglioni S, Mossini R, Falautano M, Scotti G, et al. 2006. The contribution of voxel-based morphometry in staging patients with mild cognitive impairment. Neurology. 67:453–460.

Bressler SL, Menon V. 2010. Large-scale brain networks in cognition: emerging methods and principles. Trends Cogn Sci. 14:277–290.

Broyd SJ, Demanuele C, Debener S, Helps SK, James CJ, Sonuga-Barke EJ. 2009. Default-mode brain dysfunction in mental disorders: a systematic review. Neurosci Biobehav Rev. 33: 279–296.

Buckner RL, Andrews-Hanna JR, Schacter DL. 2008. The brain's default network: anatomy, function, and relevance to disease. Ann NY Acad Sci. 1124:1–38.

Buckner RL, Sepulcre J, Talukdar T, Krienen FM, Liu H, Hedden T, Andrews-Hanna JR, Sperling RA, Johnson KA. 2009. Cortical hubs revealed by intrinsic functional connectivity: mapping, assessment of stability, and relation to Alzheimer's disease. J Neurosci. 29:1860–1873.

Bullmore E, Sporns O. 2012. The economy of brain network organization. Nat Rev Neurosci. 13:336–349.

Butefisch CM, Davis BC, Wise SP, Sawaki L, Kopylev L, Classen J, Cohen LG. 2000. Mechanisms of use-dependent plasticity in the human motor cortex. Proc Natl Acad Sci USA. 97:3661–3665.

Catani M, ffytche DH. 2005. The rises and falls of disconnection syndromes. Brain. 128:2224–2239.

Cole MW, Reynolds JR, Power JD, Repovs G, Anticevic A, Braver TS. 2013. Multi-task connectivity reveals flexible hubs for adaptive task control. Nat Neurosci. 16:1348–1355.

Crossley NA, Mechelli A, Scott J, Carletti F, Fox PT, McGuire P, Bullmore ET. 2014. The hubs of the human connectome are generally implicated in the anatomy of brain disorders. Brain. 137:2382–2395.

Dai Z, Yan C, Li K, Wang Z, Wang J, Cao M, Lin Q, Shu N, Xia M, Bi Y, et al. 2015. Identifying and mapping connectivity patterns of brain network hubs in Alzheimer's disease. Cereb Cortex. 25:3723–3742.

Damaraju E, Allen EA, Belger A, Ford JM, McEwen S, Mathalon DH, Mueller BA, Pearlson GD, Potkin SG, Preda A, et al. 2014. Dynamic functional connectivity analysis reveals transient states of dysconnectivity in schizophrenia. Neuroimage Clin. 5:298–308.

de Haan W, van der Flier WM, Koene T, Smits LL, Scheltens P, Stam CJ. 2012. Disrupted modular brain dynamics reflect cognitive dysfunction in Alzheimer's disease. Neuroimage. 59:3085–3093.

Deco G, Jirsa VK, McIntosh AR. 2011. Emerging concepts for the dynamical organization of resting-state activity in the brain. Nat Rev Neurosci. 12:43–56.

Duan H, Wearne SL, Morrison JH, Hof PR. 2002. Quantitative analysis of the dendritic morphology of corticocortical projection neurons in the macaque monkey association cortex. Neuroscience. 114:349–359.

Eickhoff SB, Bzdok D, Laird AR, Kurth F, Fox PT. 2012. Activation likelihood estimation meta-analysis revisited. Neuroimage. 59:2349–2361.

Faivre A, Rico A, Zaaraoui W, Crespy L, Reuter F, Wybrecht D, Soulier E, Malikova I, Confort-Gouny S, Cozzone PJ. 2012.

Assessing brain connectivity at rest is clinically relevant in early multiple sclerosis. Mult Scler. 18:1251–1258.
Filippi M, van den Heuvel MP, Fornito A, He Y, Hulshoff Pol HE, Agosta F, Comi G, Rocca MA. 2013. Assessment of system dysfunction in the brain through MRI-based connectomics. Lancet Neurol. 12:1189–1199.
Fornito A, Zalesky A, Breakspear M. 2015. The connectomics of brain disorders. Nat Rev Neurosci. 16:159–172.
Fox MD, Buckner RL, Liu H, Chakravarty MM, Lozano AM, Pascual-Leone A. 2014. Resting-state networks link invasive and noninvasive brain stimulation across diverse psychiatric and neurological diseases. Proc Natl Acad Sci USA. 111:E4367–E4375.
Fox MD, Buckner RL, White MP, Greicius MD, Pascual-Leone A. 2012. Efficacy of transcranial magnetic stimulation targets for depression is related to intrinsic functional connectivity with the subgenual cingulate. Biol Psychiatry. 72:595–603.
Fox MD, Snyder AZ, Vincent JL, Corbetta M, Van Essen DC, Raichle ME. 2005. The human brain is intrinsically organized into dynamic, anticorrelated functional networks. Proc Natl Acad Sci USA. 102:9673–9678.
Frodl T, Koutsouleris N, Bottlender R, Born C, Jager M, Morgenthaler M, Scheuerecker J, Zill P, Baghai T, Schule C, et al. 2008. Reduced gray matter brain volumes are associated with variants of the serotonin transporter gene in major depression. Mol Psychiatry. 13:1093–1101.
Gong Q, He Y. 2015. Depression, neuroimaging and connectomics: a selective overview. Biol Psychiatry. 77:223–235.
Gratton C, Nomura EM, Perez F, D'Esposito M. 2012. Focal brain lesions to critical locations cause widespread disruption of the modular organization of the brain. J Cogn Neurosci. 24: 1275–1285.
Groenewold NA, Opmeer EM, de Jonge P, Aleman A, Costafreda SG. 2013. Emotional valence modulates brain functional abnormalities in depression: evidence from a meta-analysis of fMRI studies. Neurosci Biobehav Rev. 37:152–163.
Guimera R, Nunes Amaral LA. 2005. Functional cartography of complex metabolic networks. Nature. 433:895–900.
Guimera R, Sales-Pardo M, Amaral LA. 2007. Classes of complex networks defined by role-to-role connectivity profiles. Nat Phys. 3:63–69.
Hagmann P, Cammoun L, Gigandet X, Meuli R, Honey CJ, Wedeen VJ, Sporns O. 2008. Mapping the structural core of human cerebral cortex. PLoS Biol. 6:e159.
Hamilton JP, Etkin A, Furman DJ, Lemus MG, Johnson RF, Gotlib IH. 2012. Functional neuroimaging of major depressive disorder: a meta-analysis and new integration of base line activation and neural response data. Am J Psychiatry. 169:693–703.
He Y, Chen Z, Evans A. 2008. Structural insights into aberrant topological patterns of large-scale cortical networks in Alzheimer's disease. J Neurosci. 28:4756–4766.
He Y, Wang J, Wang L, Chen ZJ, Yan C, Yang H, Tang H, Zhu C, Gong Q, Zang Y, et al. 2009. Uncovering intrinsic modular organization of spontaneous brain activity in humans. PLoS One. 4:e5226.
Honey CJ, Sporns O, Cammoun L, Gigandet X, Thiran JP, Meuli R, Hagmann P. 2009. Predicting human resting-state functional connectivity from structural connectivity. Proc Natl Acad Sci USA. 106:2035–2040.
Honey CJ, Thivierge JP, Sporns O. 2010. Can structure predict function in the human brain? Neuroimage. 52:766–776.
Jacobs B, Schall M, Prather M, Kapler E, Driscoll L, Baca S, Jacobs J, Ford K, Wainwright M, Treml M. 2001. Regional dendritic and spine variation in human cerebral cortex: a quantitative golgi study. Cereb Cortex. 11:558–571.
Keedy SK, Rosen C, Khine T, Rajarethinam R, Janicak PG, Sweeney JA. 2009. An fMRI study of visual attention and sensorimotor function before and after antipsychotic treatment in first-episode schizophrenia. Psychiatry Res. 172:16–23.
Kerestes R, Ladouceur CD, Meda S, Nathan PJ, Blumberg HP, Maloney K, Ruf B, Saricicek A, Pearlson GD, Bhagwagar Z, et al. 2012. Abnormal prefrontal activity subserving attentional control of emotion in remitted depressed patients during a working memory task with emotional distracters. Psychol Med. 42:29–40.
Lancaster JL, Tordesillas-Gutierrez D, Martinez M, Salinas F, Evans A, Zilles K, Mazziotta JC, Fox PT. 2007. Bias between MNI and Talairach coordinates analyzed using the ICBM-152 brain template. Hum Brain Mapp. 28:1194–1205.
Li HJ, Hou XH, Liu HH, Yue CL, He Y, Zuo XN. 2015. Toward systems neuroscience in mild cognitive impairment and Alzheimer's disease: a meta-analysis of 75 fMRI studies. Hum Brain Mapp. 36:1217–1232.
Liang X, Zou Q, He Y, Yang Y. 2013. Coupling of functional connectivity and regional cerebral blood flow reveals a physiological basis for network hubs of the human brain. Proc Natl Acad Sci USA. 110:1929–1934.
Liang X, Zou Q, He Y, Yang Y. 2016. Topologically Reorganized Connectivity Architecture of Default-Mode, Executive-Control, and Salience Networks across Working Memory Task Loads. Cereb Cortex. 26:1501–1511.
Lowe MJ, Beall EB, Sakaie KE, Koenig KA, Stone L, Marrie RA, Phillips MD. 2008. Resting state sensorimotor functional connectivity in multiple sclerosis inversely correlates with transcallosal motor pathway transverse diffusivity. Hum Brain Mapp. 29:818–827.
Lynch CJ, Uddin LQ, Supekar K, Khouzam A, Phillips J, Menon V. 2013. Default mode network in childhood autism: posteromedial cortex heterogeneity and relationship with social deficits. Biol Psychiatry. 74:212–219.
McIntyre CC, Hahn PJ. 2010. Network perspectives on the mechanisms of deep brain stimulation. Neurobiol Dis. 38:329–337.
McTeague LM, Huemer J, Carreon DM, Jiang Y, Eickhoff SB, Etkin A. 2017. Identification of common neural circuit disruptions in cognitive control across psychiatric disorders. Am J Psychiatry. 174:676–685.
Menon V. 2011. Large-scale brain networks and psychopathology: a unifying triple network model. Trends Cogn Sci. 15:483–506.
Mesulam MM. 1998. From sensation to cognition. Brain. 121(Pt 6): 1013–1052.
Meunier D, Achard S, Morcom A, Bullmore E. 2009. Age-related changes in modular organization of human brain functional networks. Neuroimage. 44:715–723.
Murphy K, Fox MD. 2017. Towards a consensus regarding global signal regression for resting state functional connectivity MRI. Neuroimage. 154:169–173.
Newman ME, Girvan M. 2004. Finding and evaluating community structure in networks. Phys Rev E Stat Nonlin Soft Matter Phys. 69:026113.
Park HJ, Friston K. 2013. Structural and functional brain networks: from connections to cognition. Science. 342:1238411.
Power JD, Barnes KA, Snyder AZ, Schlaggar BL, Petersen SE. 2012. Spurious but systematic correlations in functional connectivity MRI networks arise from subject motion. Neuroimage. 59:2142–2154.
Power JD, Cohen AL, Nelson SM, Wig GS, Barnes KA, Church JA, Vogel AC, Laumann TO, Miezin FM, Schlaggar BL, et al. 2011. Functional network organization of the human brain. Neuron. 72:665–678.

Power JD, Mitra A, Laumann TO, Snyder AZ, Schlaggar BL, Petersen SE. 2014. Methods to detect, characterize, and remove motion artifact in resting state fMRI. Neuroimage. 84:320–341.

Power JD, Schlaggar BL, Lessov-Schlaggar CN, Petersen SE. 2013. Evidence for hubs in human functional brain networks. Neuron. 79:798–813.

Purves D, Augustine GJ, Fitzpatrick D, Katz LC, LaMantia A-S, McNamara JO, Williams SM. 2001. The Association Cortices. Sunderland, MA: Sinauer.

Qin J, Liu H, Wei M, Zhao K, Chen J, Zhu J, Shen X, Yan R, Yao Z, Lu Q. 2017. Reconfiguration of hub-level community structure in depressions: a follow-up study via diffusion tensor imaging. J Affect Disord. 207:305–312.

Radua J, Mataix-Cols D, Phillips ML, El-Hage W, Kronhaus DM, Cardoner N, Surguladze S. 2012. A new meta-analytic method for neuroimaging studies that combines reported peak coordinates and statistical parametric maps. Eur Psychiatry. 27:605–611.

Radua J, Rubia K, Canales-Rodriguez EJ, Pomarol-Clotet E, Fusar-Poli P, Mataix-Cols D. 2014. Anisotropic kernels for coordinate-based meta-analyses of neuroimaging studies. Front Psychiatry. 5:13.

Raichle ME, Gusnard DA. 2002. Appraising the brain's energy budget. Proc Natl Acad Sci USA. 99:10237–10239.

Raichle ME, MacLeod AM, Snyder AZ, Powers WJ, Gusnard DA, Shulman GL. 2001. A default mode of brain function. Proc Natl Acad Sci USA. 98:676–682.

Raichle ME, Mintun MA. 2006. Brain work and brain imaging. Annu Rev Neurosci. 29:449–476.

Rioult-Pedotti MS, Friedman D, Hess G, Donoghue JP. 1998. Strengthening of horizontal cortical connections following skill learning. Nat Neurosci. 1:230–234.

Schmaal L, Hibar DP, Samann PG, Hall GB, Baune BT, Jahanshad N, Cheung JW, van Erp TG, Bos D, Ikram MA, et al. 2017. Cortical abnormalities in adults and adolescents with major depression based on brain scans from 20 cohorts worldwide in the ENIGMA Major Depressive Disorder Working Group. Mol Psychiatry. 22:900–909.

Schwarz AJ, McGonigle J. 2011. Negative edges and soft thresholding in complex network analysis of resting state functional connectivity data. Neuroimage. 55:1132–1146.

Seeley WW, Crawford RK, Zhou J, Miller BL, Greicius MD. 2009. Neurodegenerative diseases target large-scale human brain networks. Neuron. 62:42–52.

Seeley WW, Menon V, Schatzberg AF, Keller J, Glover GH, Kenna H, Reiss AL, Greicius MD. 2007. Dissociable intrinsic connectivity networks for salience processing and executive control. J Neurosci. 27:2349–2356.

Smith SM, Fox PT, Miller KL, Glahn DC, Fox PM, Mackay CE, Filippini N, Watkins KE, Toro R, Laird AR. 2009. Correspondence of the brain's functional architecture during activation and rest. Proc Natl Acad Sci USA. 106: 13040–13045.

Sporns O, Betzel RF. 2016. Modular brain networks. Annu Rev Psychol. 67:613–640.

Stam CJ. 2014. Modern network science of neurological disorders. Nat Rev Neurosci. 15:683–695.

Tomasi D, Wang GJ, Volkow ND. 2013. Energetic cost of brain functional connectivity. Proc Natl Acad Sci USA. 110: 13642–13647.

Tzourio-Mazoyer N, Landeau B, Papathanassiou D, Crivello F, Etard O, Delcroix N, Mazoyer B, Joliot M. 2002. Automated anatomical labeling of activations in SPM using a macroscopic anatomical parcellation of the MNI MRI single-subject brain. Neuroimage. 15:273–289.

van den Heuvel MP, Sporns O. 2011. Rich-club organization of the human connectome. J Neurosci. 31:15775–15786.

van den Heuvel MP, Sporns O. 2013a. An anatomical substrate for integration among functional networks in human cortex. J Neurosci. 33:14489–14500.

van den Heuvel MP, Sporns O. 2013b. Network hubs in the human brain. Trends Cogn Sci. 17:683–696.

van Hartevelt TJ, Cabral J, Deco G, Moller A, Green AL, Aziz TZ, Kringelbach ML. 2014. Neural plasticity in human brain connectivity: the effects of long term deep brain stimulation of the subthalamic nucleus in Parkinson's disease. PLoS One. 9:e86496.

van Tol MJ, van der Wee NJ, van den Heuvel OA, Nielen MM, Demenescu LR, Aleman A, Renken R, van Buchem MA, Zitman FG, Veltman DJ. 2010. Regional brain volume in depression and anxiety disorders. Arch Gen Psychiatry. 67:1002–1011.

Wang J, Zuo X, Dai Z, Xia M, Zhao Z, Zhao X, Jia J, Han Y, He Y. 2013. Disrupted functional brain connectome in individuals at risk for Alzheimer's disease. Biol Psychiatry. 73:472–481.

Wang J, Zuo X, He Y. 2010. Graph-based network analysis of resting-state functional MRI. Front Syst Neurosci. 4:16.

Wang K, Liang M, Wang L, Tian L, Zhang X, Li K, Jiang T. 2007. Altered functional connectivity in early Alzheimer's disease: a resting-state fMRI study. Hum Brain Mapp. 28:967–978.

Wang Z, Dai Z, Gong G, Zhou C, He Y. 2015. Understanding structural-functional relationships in the human brain: a large-scale network perspective. Neuroscientist. 21:290–305.

Warren DE, Power JD, Bruss J, Denburg NL, Waldron EJ, Sun H, Petersen SE, Tranel D. 2014. Network measures predict neuropsychological outcome after brain injury. Proc Natl Acad Sci USA. 111:14247–14252.

Weil RS, Schrag AE, Warren JD, Crutch SJ, Lees AJ, Morris HR. 2016. Visual dysfunction in Parkinson's disease. Brain. 139: 2827–2843.

Wu T, Wang L, Chen Y, Zhao C, Li K, Chan P. 2009. Changes of functional connectivity of the motor network in the resting state in Parkinson's disease. Neurosci Lett. 460:6–10.

Xia M, Wang J, He Y. 2013. BrainNet viewer: a network visualization tool for human brain connectomics. PLoS One. 8: e68910.

Yeo BT, Krienen FM, Eickhoff SB, Yaakub SN, Fox PT, Buckner RL, Asplund CL, Chee MW. 2016. Functional specialization and flexibility in human association cortex. Cereb Cortex. 26:465.

Yeo BT, Krienen FM, Sepulcre J, Sabuncu MR, Lashkari D, Hollinshead M, Roffman JL, Smoller JW, Zollei L, Polimeni JR, et al. 2011. The organization of the human cerebral cortex estimated by intrinsic functional connectivity. J Neurophysiol. 106:1125–1165.

Yoon S, Kim JE, Hwang J, Kim TS, Kang HJ, Namgung E, Ban S, Oh S, Yang J, Renshaw PF, et al. 2016. Effects of creatine monohydrate augmentation on brain metabolic and network outcome measures in women with major depressive disorder. Biol Psychiatry. 80:439–447.

Zang Y, He Y, Zhu C, Cao Q, Sui M, Liang M, Tian L, Jiang T, Wang Y. 2007. Altered baseline brain activity in children with ADHD revealed by resting-state functional MRI. Brain Dev. 29:83–91.

Zang Y, Jiang T, Lu Y, He Y, Tian L. 2004. Regional homogeneity approach to fMRI data analysis. Neuroimage. 22:394–400.

Zhang J, Wang J, Wu Q, Kuang W, Huang X, He Y, Gong Q. 2011. Disrupted brain connectivity networks in drug-naive, first-episode major depressive disorder. Biol Psychiatry. 70: 334–342.